

Thoresen, H.E., Cassel, E.J., Smith, M.E., Stockli D.F., Jicha, B.R., 2024, Stratigraphic and geochronologic investigation of the Muddy Creek Basin: Implications for the Eocene tectonic evolution of southwest Montana, USA: GSA Bulletin, <https://doi.org/10.1130/B37268.1>.

## Supplemental Material

**Supplemental Text S1.** Full analytical methods.

**Figure S1.** Detrital zircon maximum depositional age calculations exported from DetritalPy.

**Figure S2.** Maximum likelihood age calculations exported from IsoPlotR.

**Figure S3.** Summary plots of sanidine  $^{40}\text{Ar}/^{39}\text{Ar}$  analyses.

**Figures S4-S12.** Measured stratigraphic sections.

**Table S1.** Detrital zircon U-Pb data tables.

**Table S2.** Sanidine  $^{40}\text{Ar}/^{39}\text{Ar}$  data tables.

**Table S3.** (U-Th)/He data tables from the University of Connecticut BAHTL lab.

**Table S4.** (U-Th)/He data tables from the University of Texas, Austin UTChron lab.

**Table S5.** Summary table of complete Muddy Creek Basin section with thickness and hypothesized lithologies of missing section.

## **Zircon (U-Pb) Geochronology**

*These methods are provided by the UTChron Lab at the University of Texas, Austin.* U-Pb geochronology was conducted at the laser ablation high-resolution inductively coupled plasma mass spectrometry laboratory at the University of Texas at Austin (UTChron Laboratory, Department of Geological Sciences). The LA-ICP-MS system consisted of a Photon Machines Analyte.G2 ArF excimer 193nm laser, equipped with a two-volume Helex sample cell, coupled to a Thermo Element 2 double-focusing magnetic sector ICP-MS. Helium was used as the carrier gas and mixed with Argon before entering the ICPMS. Laser ablation depth profiling was carried out on zircon grains sprinkled onto double-sided tape with a laser beam diameter of 25-30µm, operated with an energy density of 1.5-2.5 J/cm<sup>2</sup> measured with an energy meter, and a pulse rate of 10 Hz. Each analysis consisted of 4 cleaning shots, 25 seconds of baseline data collection, 30 seconds of ablation, and 30 seconds of washout. Ablation rates of ~0.5µm/second mean that only the outer 15-17µm of zircons are typically sampled by this technique.

Elemental and isotopic fractionation are corrected by interspersed analysis of primary zircon standard GJ1 (<sup>206</sup>Pb/<sup>238</sup>U age = 601.7 ± 1.3 Ma; Jackson et al., 2004). Analyses were made in repeating blocks of one standard followed by 5 unknowns, with Plesovice zircon (<sup>206</sup>Pb/<sup>238</sup>U age = 337.13±0.37 Ma; Slama et al., 2008), and Pak1 zircon (<sup>206</sup>Pb/<sup>238</sup>U age = 43.0 ±0.01 Ma; NIGL TIMS) measured for quality control. Uncertainty resulting from calibration correction is generally 1-2% for both <sup>206</sup>Pb/<sup>207</sup>Pb and <sup>206</sup>Pb/<sup>238</sup>U. Age calculations were performed using Iolite3.7 (Paton et al., 2011) and VizualAge (Petrus and Kamber, 2012), from baseline-subtracted intensities. No correction was applied for common Pb due to interferences in measurement of <sup>204</sup>Pb; however common Pb was evaluated graphically and high Pb zones usually rejected. U-Pb data were plotted using DetritalPy (Sharman et al., 2018). Errors for isotopic ratios and ages are presented as 2-sigma absolute errors.

## **Zircon (U-Th)/He Thermochronology**

*These methods are provided by BAHTL at the University of Connecticut.*

### *Data Collection*

Zircon crystals from samples are hand-picked, screened, and photographed under ethyl alcohol at 120x magnification and cross-polarized light using a Leica M165 binocular microscope equipped with a calibrated digital camera. Selected crystals are screened for quality, crystal size, shape, and the absence of inclusions. Crystal size measurements of selected grains are collected from these high-resolution images to calculate crystal mass and alpha-ejection correction factors used in the (U-Th-Sm)/He age analysis. Individual crystals are then transferred into 1 mm diameter Nb foil packets for stable heating during gas extraction.

Nb packets containing the mineral aliquots are loaded into the He gas extraction line and pumped down to high vacuum (<10<sup>-8</sup> torr). Packets are then heated with a diode laser at 1200°C for 15 minutes to extract radiogenic <sup>4</sup>He. Sample gas is spiked with ~7 ncc of pure <sup>3</sup>He, cleaned using two SAES getters and cryogenic purification, and analyzed on a Balzers PrismaPlus QME 220 quadrupole mass spectrometer. This gas extraction and measurement procedure was repeated at least once to ensure complete mineral degassing to <2% re-extract gas volume. Aliquot <sup>4</sup>He gas concentrations are calculated from these data.

Degassed aliquots are shipped to the University of Colorado Thermochronology Research and Instrumentation Laboratory (TRaIL) for chemical dissolution and U-Th measurement. At TRaIL,

zircon grains are dissolved using Parr large-capacity dissolution vessels in a multi-step acid-vapor dissolution process. Grains (including the Nb tube) are placed in Ludwig-style Savillex vials, spiked with a  $^{235}\text{U} - ^{230}\text{Th} - ^{145}\text{Nd}$  tracer, and mixed with 200  $\mu\text{l}$  of Optima grade HF. The vials are then capped, stacked in a 125 mL Teflon liner, placed in a Parr dissolution vessel, and baked at 220°C for 72 hours. After cooling, the vials are uncapped and dried down on a  $\sim 90^\circ\text{C}$  hot plate until dry. The vials then undergo a second round of acid-vapor dissolution, this time with 200  $\mu\text{l}$  of Optima grade HCl in each vial that is baked at 200°C for 24 hours. Vials are then dried down a second time on a hot plate. Once dry, 200  $\mu\text{l}$  of a 7:1  $\text{HNO}_3\text{:HF}$  mixture is added to each vial, the vial is capped, and cooked on the hot plate at  $\sim 90^\circ\text{C}$  for 4 hours. Once the minerals are dissolved, regardless of the dissolution process, they were diluted with 1 to 3 mL of doubly-deionized water, and taken to the ICP-MS lab for analysis. Sample solutions, along with normal solutions and blanks, were analyzed for U and Th content using a Thermo Element 2 magnetic sector mass spectrometer equipped with a Teflon spray chamber and platinum cones.

#### *Age calculations and $F_T$ corrections*

U and Th measurements from TRaIL are combined with blank-corrected He concentrations and associated grain morphometric data to calculate (U-Th)/He dates using BAHTL in-house data reduction MATLAB and Excel code.

Crystal morphometrics, crystal mass, and  $F_T$  corrections are calculated following Ketcham et al. (2011) for mean alpha stopping distances and mineral densities for a tetragonal crystal geometry.  $F_T$  is calculated for each parent isotope and applied separately in the age equation (Ketcham et al., 2011), and the reported  $F_T$  is the weighted mean value following the methods of Cooperdock et al. (2019). The reported equivalent spherical radius is derived from a surface-area/volume equivalent sphere. Effective uranium concentration (eU, ppm) is calculated as  $\text{eU} = [\text{U}] + 0.235[\text{Th}]$  after Cooperdock et al. (2019).

Analytical data and corrected dates are reported at  $\pm 1\sigma$  uncertainty. For instrument calibration and data quality-control, we routinely analyze procedural blanks and mineral standards (Durango Apatite and Fish Canyon Tuff Zircon). Long-term averages of Fish Canyon Tuff zircon analyzed in the BAHTL are  $27.7 \pm 0.5 \text{ Ma}$  ( $\pm 1\sigma$ ,  $n = 72$ ).

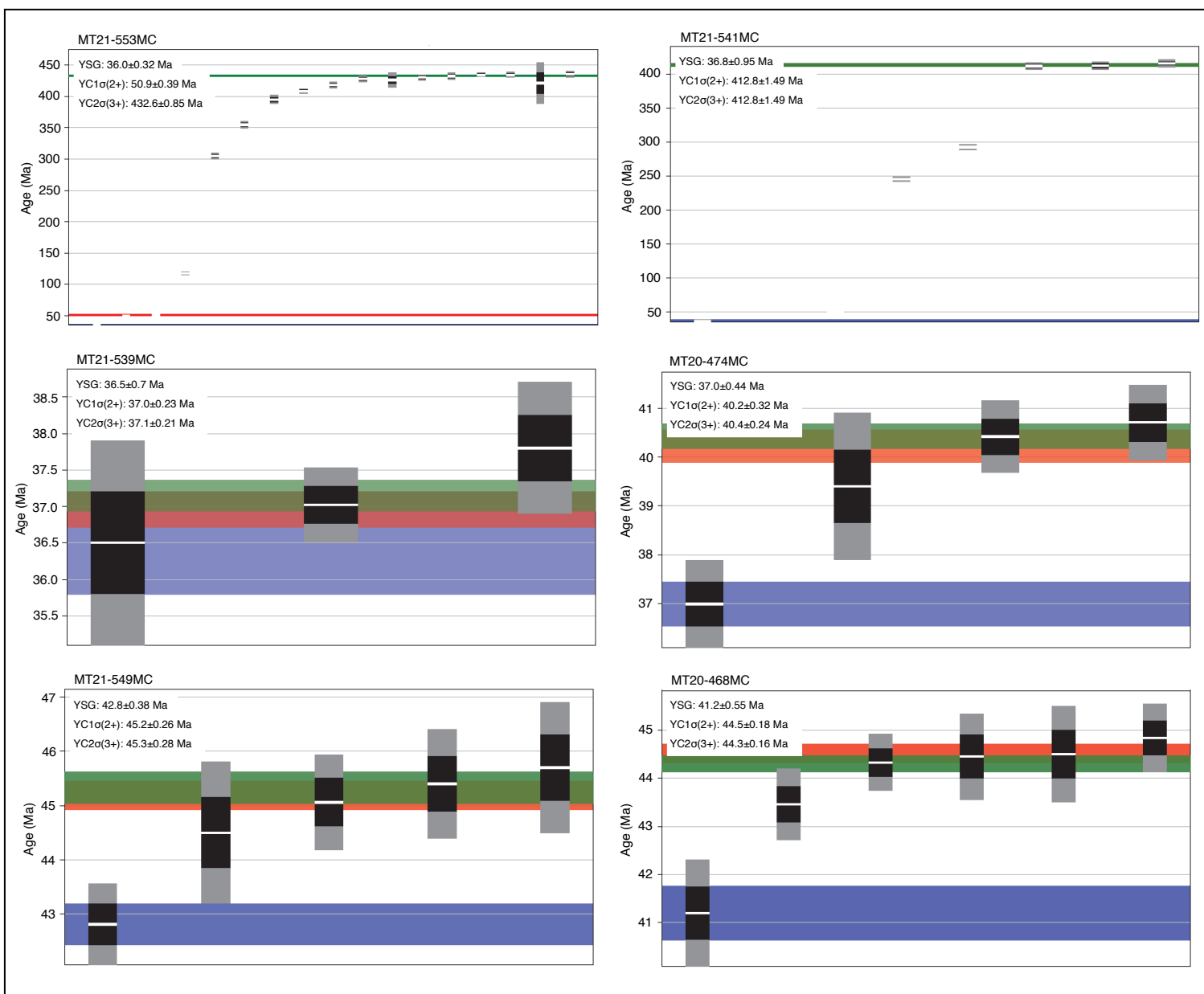


**Figure S1:** Summary figure of all maximum depositional age (MDA) calculations from the Muddy Creek Basin, modified from DetritalPy (Sharman et al., 2018). Calculated uncertainties are reported at the 1σ level. Blue band: Grain(s) included for youngest single grain (YSG); Red band: Grains included for youngest cluster of two or more grains within 1σ error (YC1σ(2+)); Green band: Grains included for youngest cluster of three or more grains within 2σ error (YC2σ(3+)); Black error bars: 1σ error; Gray error bars: 2σ error (Dickinson and Gehrels, 2009; Sharman et al., 2018).

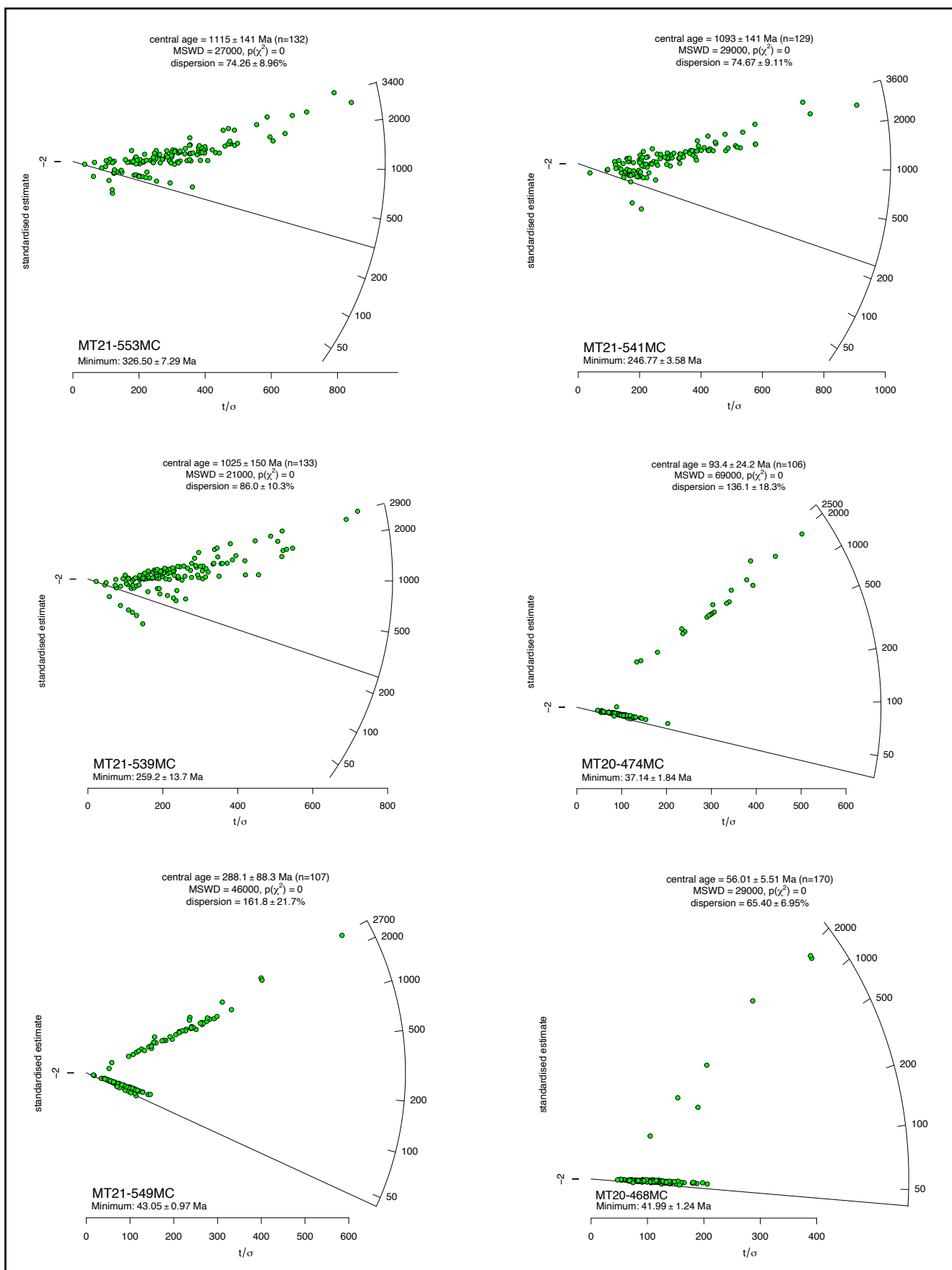


**Figure S2:** Summary figure of all maximum likelihood age (MLA) calculations from the Muddy Creek Basin, modified from IsoPlotR (Vermeesch, 2018; Vermeesch, 2021). Calculated uncertainties are reported at the  $2\sigma$  level.

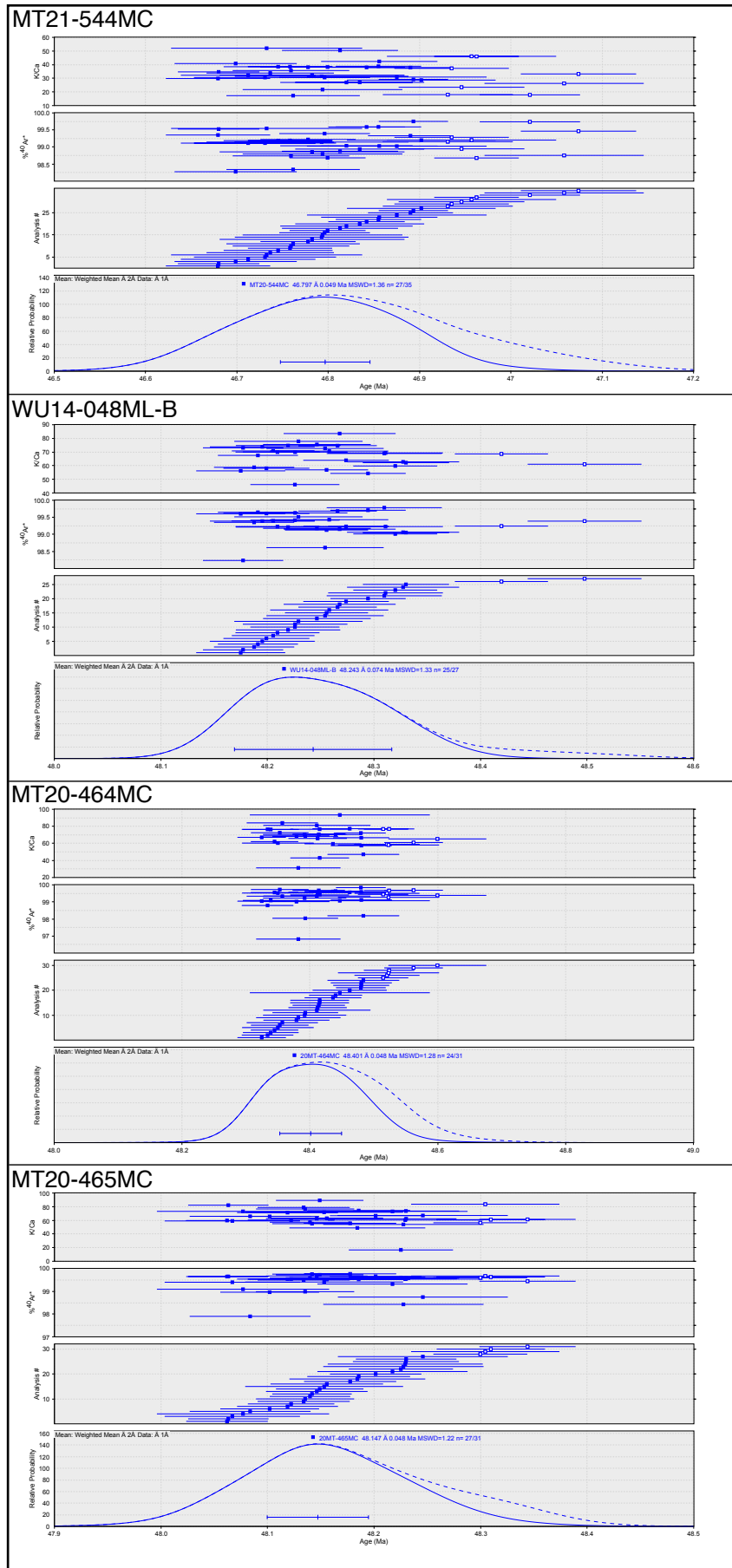


**Figure S3:** Summary plots of sanidine  $^{40}\text{Ar}/^{39}\text{Ar}$  dates from the Muddy Creek Basin. Open circles are analyses that are excluded from weighted mean calculation. Weighted mean ages have  $2\sigma$  error. MSWD: Mean standard weighted deviates.

**Table S5:** Summary table of entire Muddy Creek Basin section, including thicknesses, hypothesized lithology in missing sections, reason for missing section, and location of digitized stratigraphic column. Sections are listed in ascending stratigraphic order.

Section Name	Thickness (m)	Location of Column	Explanation
Section 19	53.8	Fig. S12	-
Missing Section	50	-	<i>Likely lacustrine mudstone with interbedded sandstone and conglomerate. Inaccessible due to erosion and private land</i>
Section 18	53.8	Fig. S11	-
Section 17	33.6	Fig. S10	-
Section 13-16	31	Fig. S9	-
		<i>2m of overlap between measured sections</i>	
Section 12	25.2	Fig. S8	-
Section 10	46.2	Fig. S7	-
		<i>3m of overlap between measured sections</i>	
Section 4-9	63	Fig. S6	-
Missing Section	100	-	<i>Likely composed of mudstone and bentonite. Inaccessible due to poor exposure and private property.</i>
Section 3	28.6	Fig. S5	-
Missing Section	30	-	<i>Likely composed of mudstone and interbedded reworked Challis Volcanics. Inaccessible due to poor exposure.</i>
Limestone Bed	3	-	Fossiliferous limestone with gastropods and stromatolites.
Missing Section	12	-	<i>Likely composed of mudstone and interbedded bentonite.</i>
Section 11	27.3	Fig. S4	-
Missing Section	129	-	<i>Likely composed of reworked Challis sediment with some interbedded mudstone.</i>
Challis Ignimbrite	9	-	Biotite-rich Challis ignimbrite.
Missing Section	53	-	<i>Inaccessible due to poor exposure.</i>
Section 1-2	34	Fig. S3	-
Missing Section	42	-	<i>Likely composed of additional Challis ignimbrites and reworked Challis sediment. Inaccessible due to poor exposure.</i>
Challis Ignimbrite	5.4	-	Basal Challis Ignimbrite, biotite rich with outsize granule lithics.
<b>Total Thickness = 829.9 m</b>			

**Figs. S4-S12:** Decimeter-scale stratigraphic sections with key provided below. All sections are at the same scale, and correlation lines are shown.

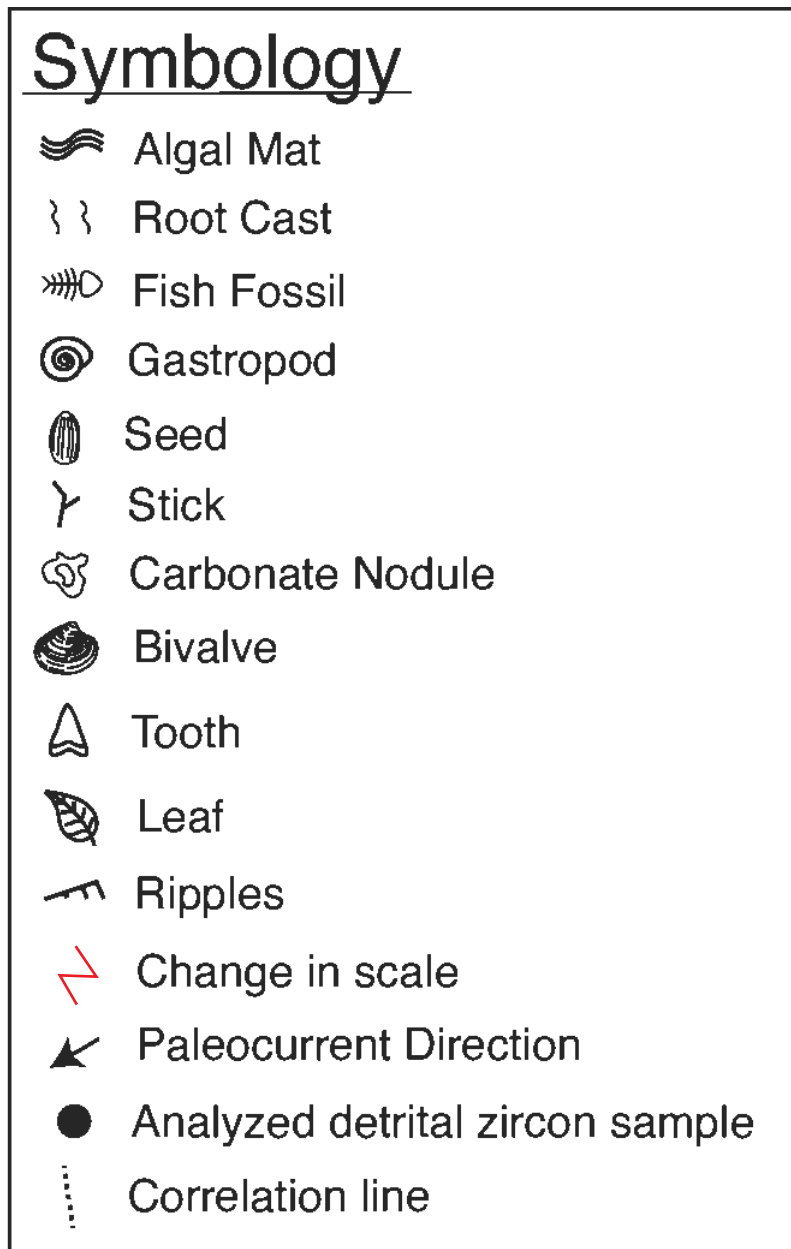
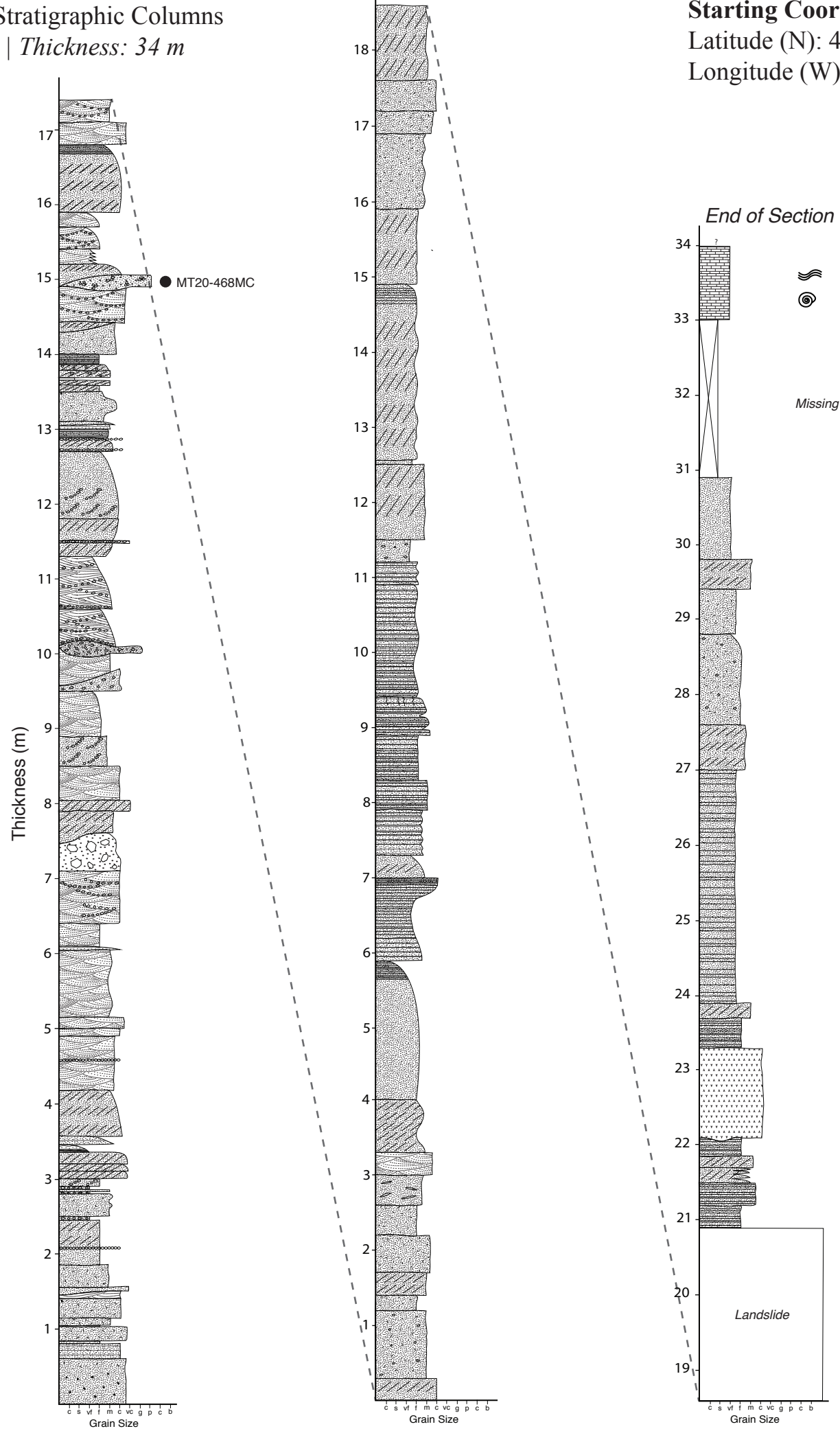


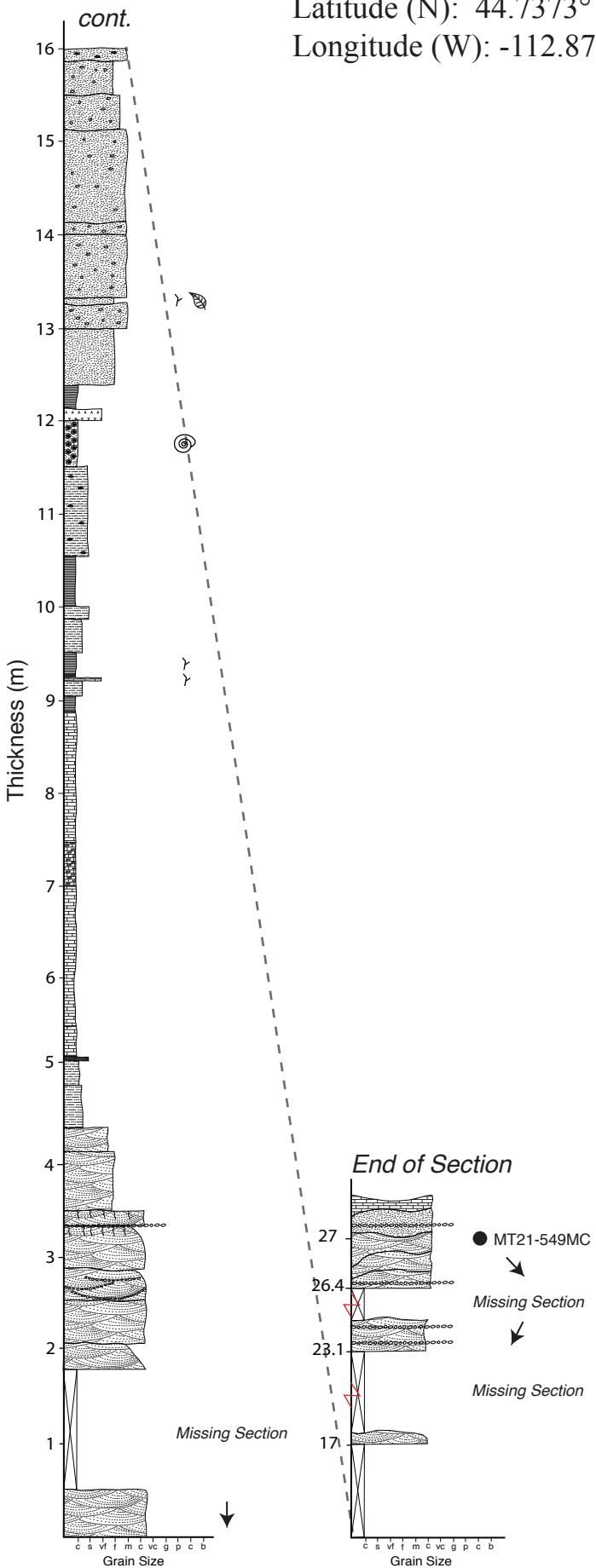


**Figure S4: Stratigraphic Columns**  
*Sections 1-2 | Thickness: 34 m*

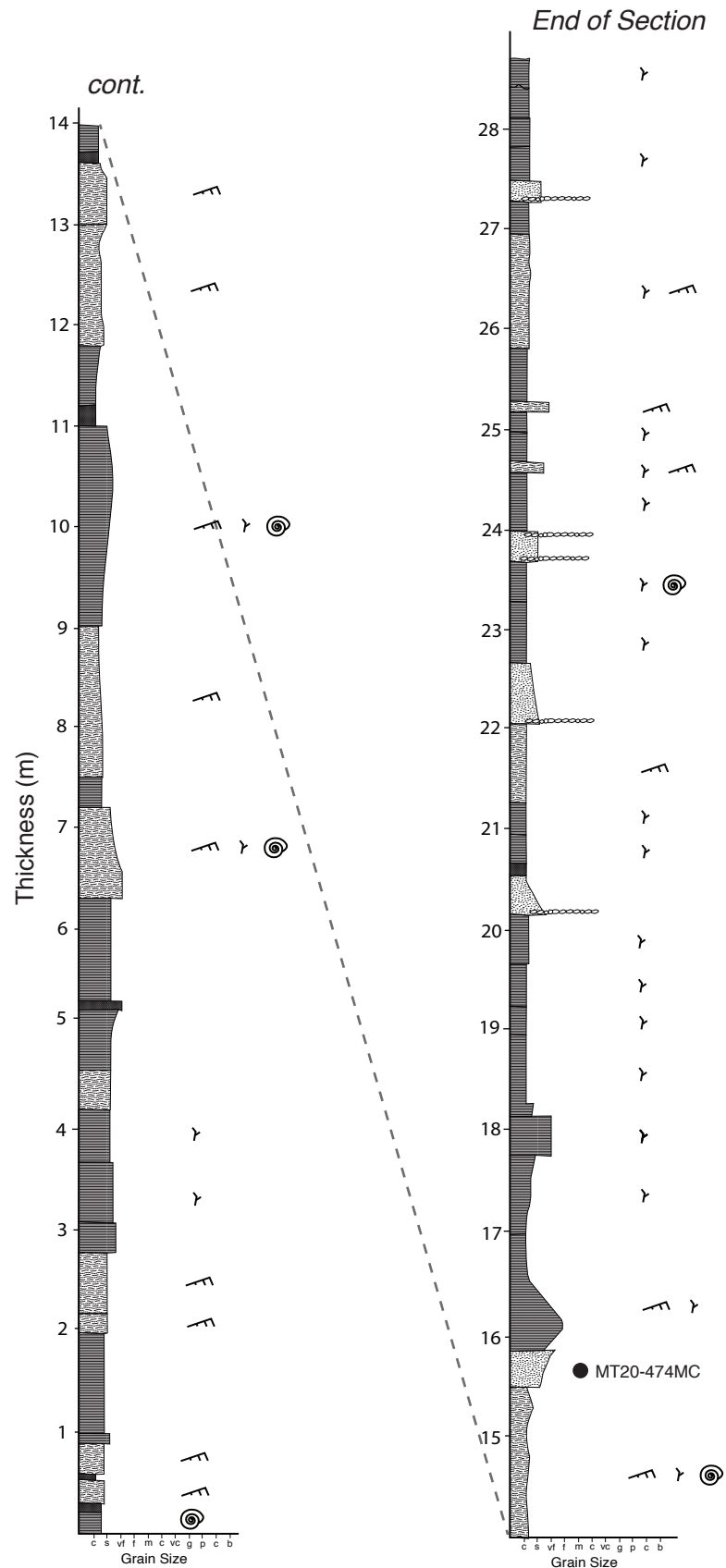


## Section 3 | Thickness: 28.6 m

Longitude (W): -112.8749°

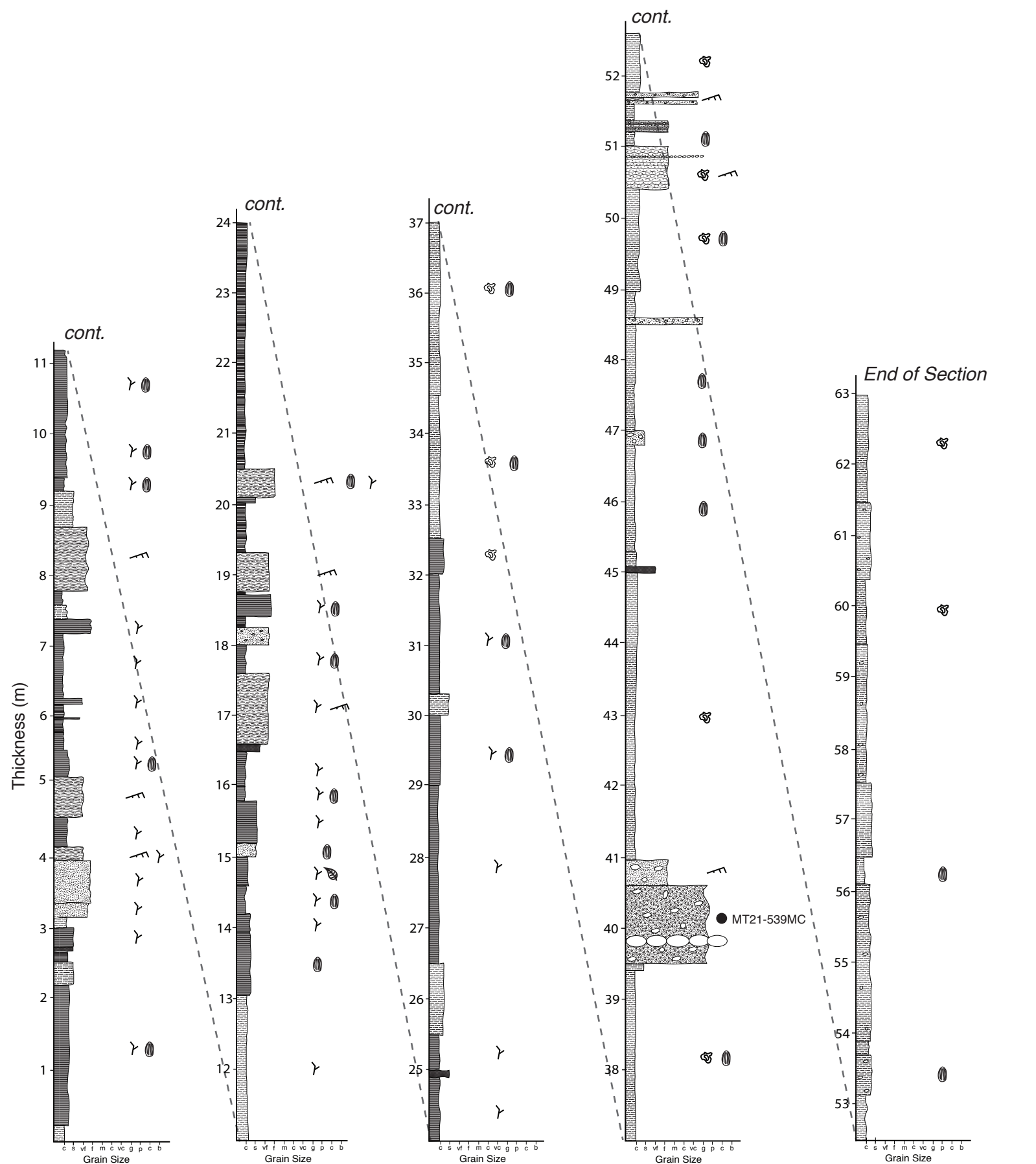


Longitude (W): -112.8587°



**Figure S6: Stratigraphic Columns**  
Section 4-9 | Thickness: 63 m

**Starting Coordinates:**  
Latitude (N): 44.6678°  
Longitude (W): -112.8350°



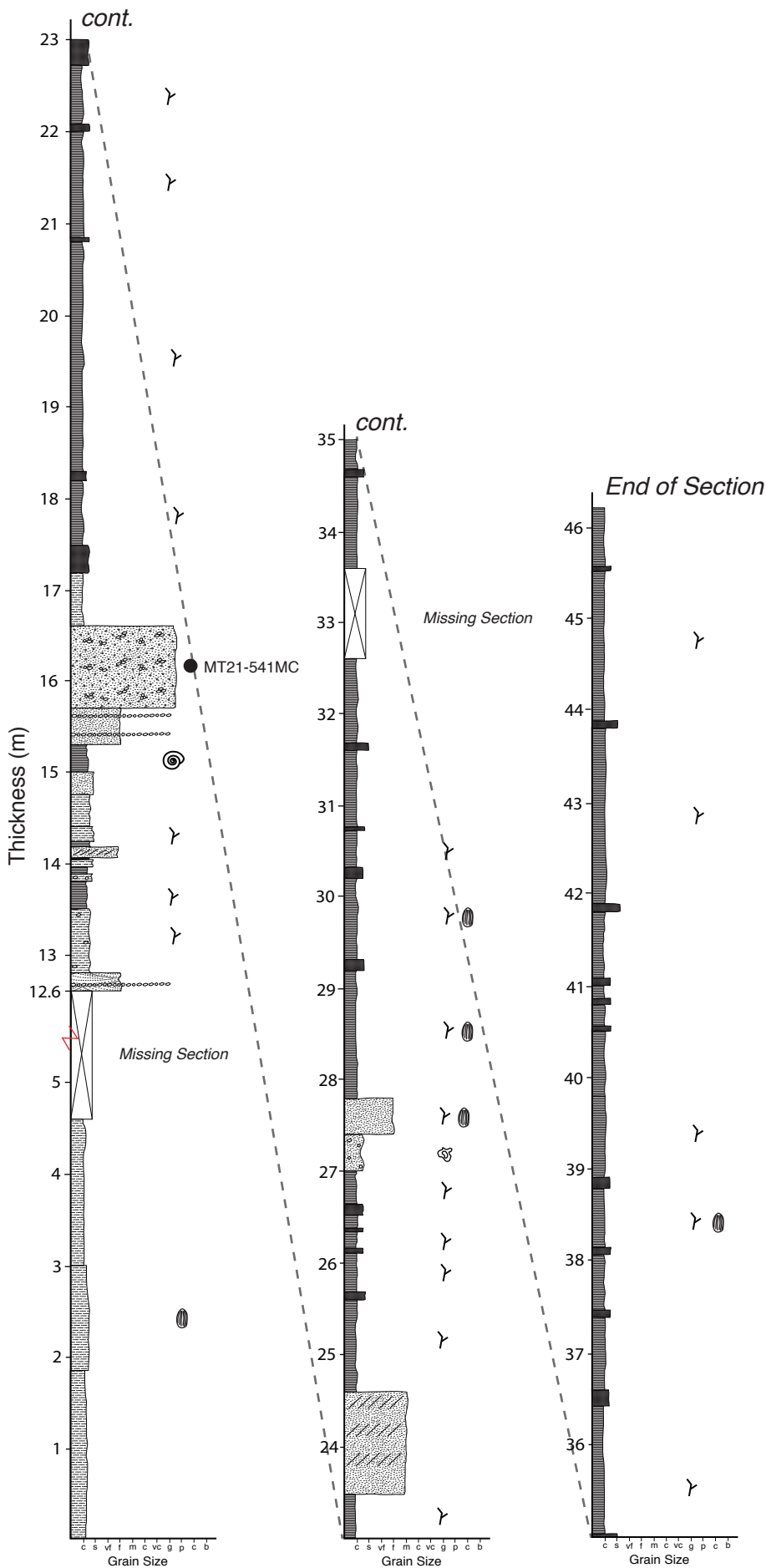


**Figure S8: Stratigraphic Columns**  
*Section 12 | Thickness: 25.2 m*

**Starting Coordinates:**  
Latitude (N): 44.6769°  
Longitude (W):-112.8365°

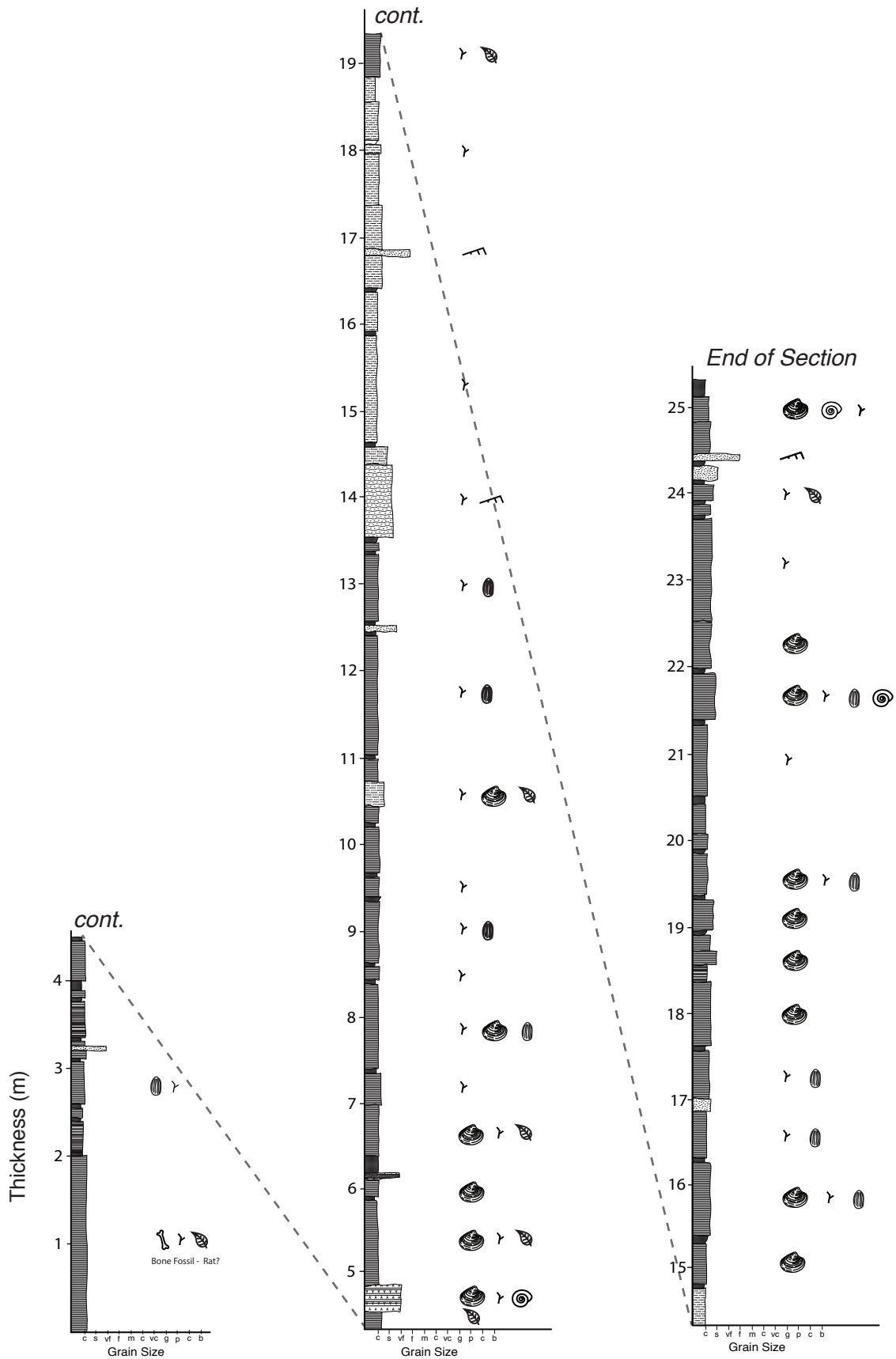


**Figure S9: Stratigraphic Columns**  
*Section 13-16 | Thickness: 31 m*

**Starting Coordinates:**  
Latitude (N): 44.6699°  
Longitude (W):-112.8335°

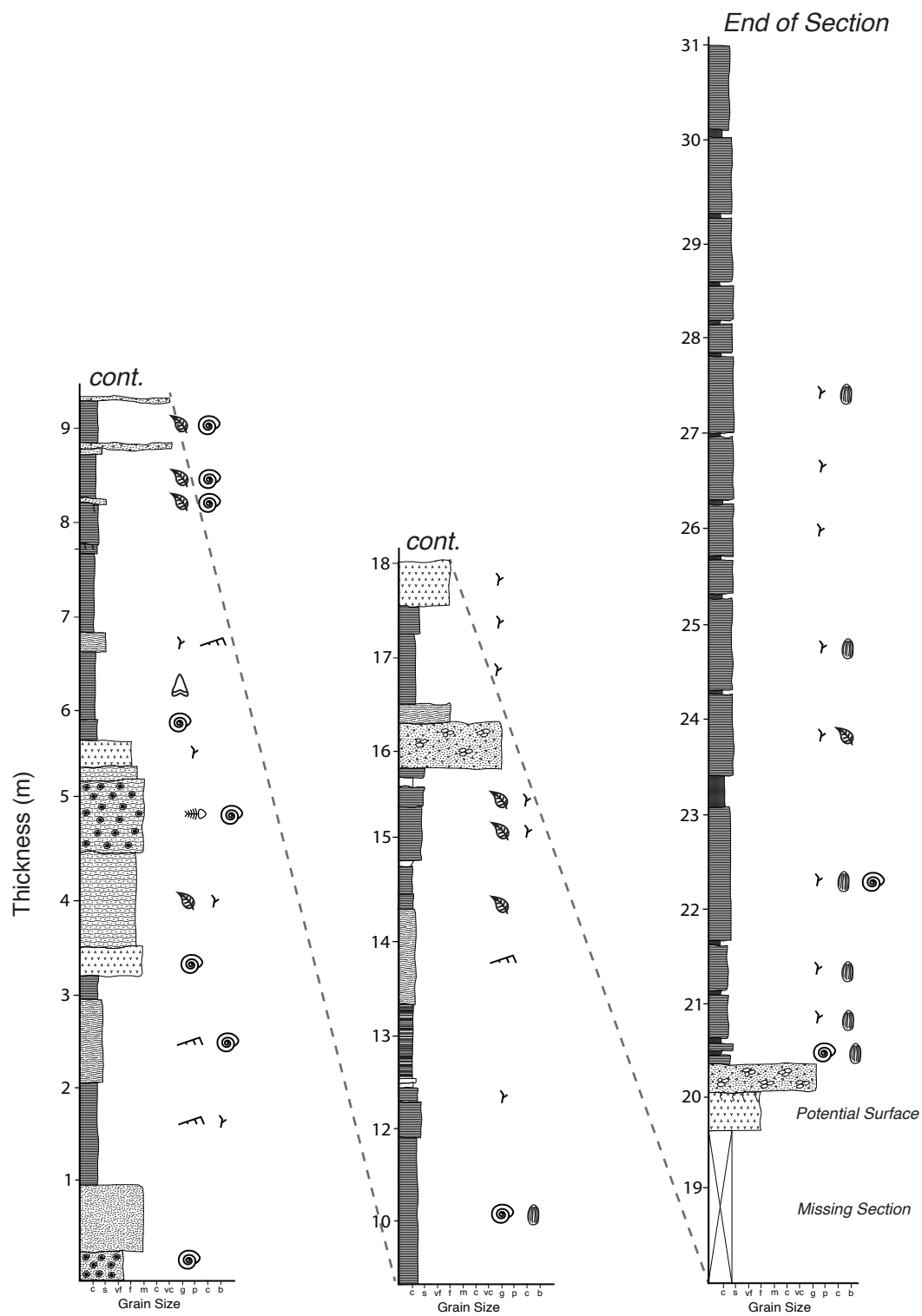


**Figure S10: Stratigraphic Columns**  
*Section 17 | Thickness: 33.6 m*

**Starting Coordinates:**  
Latitude (N): 44.6706°  
Longitude (W): -112.8324°

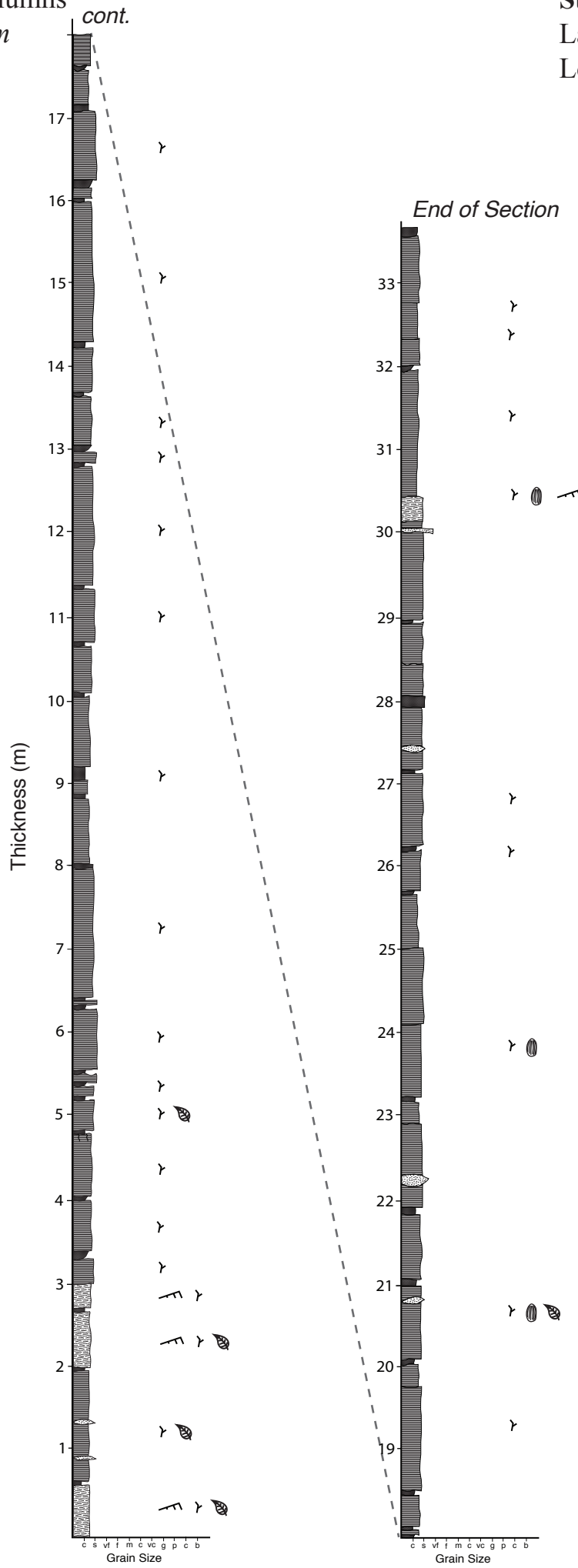


**Figure S11: Stratigraphic Columns**  
*Section 18 | Thickness: 53.8 m*

**Starting Coordinates:**  
Latitude (N): 44.6565°  
Longitude (W): -112.8217°

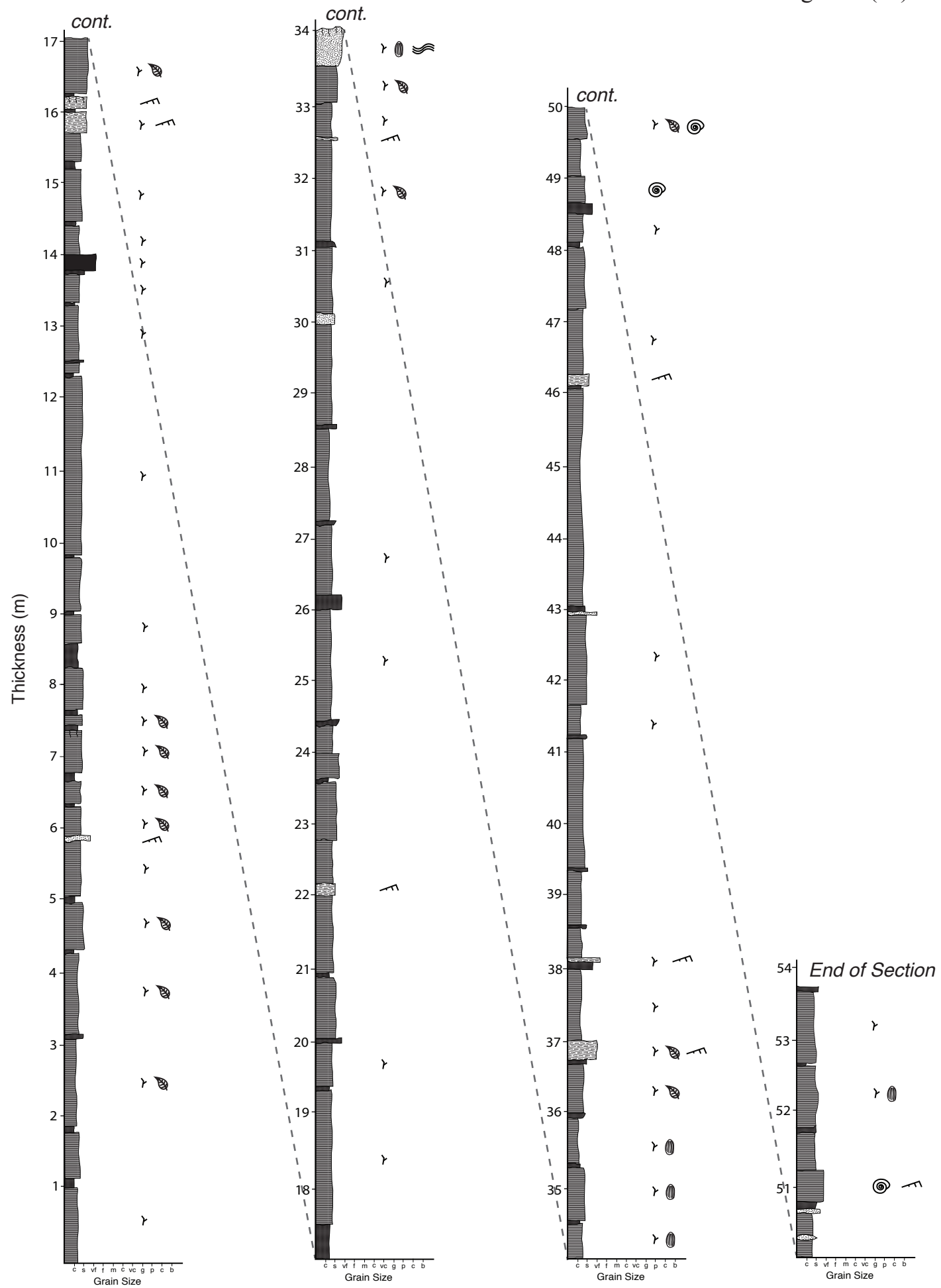




**Figure S12: Stratigraphic Columns**  
*Section 19 | Thickness: 53.8 m*

**Starting Coordinates:**  
Latitude (N): 44.6422°  
Longitude (W): -112.8105°

